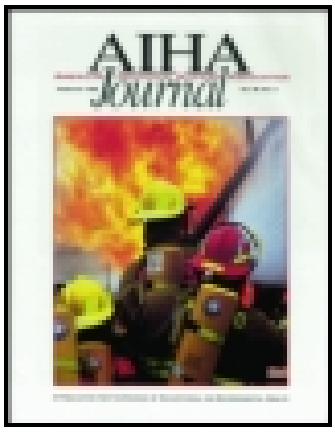

American Industrial Hygiene Association Journal
Publication details, including instructions for authors and subscription information:
http://www.tandfonline.com/loi/aiha20

Finite Difference Methods for Computation of Flow into Local Exhaust Hoods

MAZEN Y. ANASTAS [a] & ROBERT T. HUGHES [a]
[a] National Institute for Occupational Safety and Health, 4676 Columbia Parkway, Cincinnati, OH 45226
Published online: 04 Jun 2010.

To cite this article: MAZEN Y. ANASTAS & ROBERT T. HUGHES (1989) Finite Difference Methods for Computation of Flow into Local Exhaust Hoods, American Industrial Hygiene Association Journal, 50:10, 526-534, DOI: 10.1080/15298668991375119

To link to this article: http://dx.doi.org/10.1080/15298668991375119

Am. Ind. Hyg. Assoc. J. 50(10):526-534 (1989)

Finite Difference Methods for Computation of Flow into Local Exhaust Hoods

MAZEN Y. ANASTAS and ROBERT T. HUGHES
National Institute for Occupational Safety and Health, 4676 Columbia Parkway, Cincinnati, OH 45226

Local exhaust hoods play an important role in controlling exposures. Airflow into these hoods may be approximated by Laplace's equation. Previous experimental work by other authors along with other data tend to support this assumption. Currently, theoretical models are available for computing the flow into plain and flanged slots and flanged rectangles and circles. These models are analytical solutions of Laplace's equation and are possible because the velocity potentials at a given point in space can be calculated. As the geometry of configurations under study becomes more complex, closed-form solutions to Laplace's equation become more difficult to find. In such situations numerical methods of solution are called for. A finite difference method for computing the airflow is presented and was developed using the plain and flanged slot configurations. The method generally is useful for solving problems in which the location and shape of the flow boundary and the values of the velocity potential or its normal derivative are known. The analytical models for the slot were used to determine the accuracy of the numerical methods by comparison of the equal velocity contours generated by the various models. Good general agreement between the numerical solutions and analytical models was observed.

Introduction

Local exhaust ventilation plays an important role in the control of emissions and in the prevention of harmful exposures to workers in many industrial processes. Designers of these systems have used centerline models for the design of relatively simple configurations and relied on prior experience for the more complex ones. Empirical centerline velocity models for the flanged and plain basic openings (circle and rectangle) were developed by Dalla Valle[1] and by Silverman.[2,3] These models are reported in the American Conference of Governmental Industrial Hygienists'(ACGIH) industrial ventilation manual.[4] The centerline models can predict the capture characteristics of a simple hood along the centerline only. This is not sufficient to define the capture characteristics of a hood.

The availability of accurate and detailed models for the airflow into any given local exhaust hood enables the designer to qualitatively or quantitatively determine the capture characteristics thereof. This was demonstrated by Heinsohn[5] when he studied the capture characteristics of flanged and unflanged slots with respect to particulate matter. He used theoretical flow models, based in potential flow theory, as a first step in determining the capture efficiency. For these reasons there is heightened interest in predicting the air velocities induced by the various openings as a first step toward predicting their control effectiveness.

The first airflow modeling effort was performed by Tyaglo and Shepelev[6] for infinitely flanged rectangles. They derived equations for the three components of air velocity and these were related to the average velocity through the face and the values of the coordinates at a point in space. The validity of the model was verified experimentally using a rectangular hood of aspect ratio (AR) equal to 0.1. Aspect ratio is defined as the ratio of width to length of a rectangle. Good agreement between experimental and theoretical centerline velocities was found.

A potential flow model for an infinitely flanged circular hood was derived by Drkal[7] and published about the same time as Tyaglo and Shepelev's model for the rectangle. Centerline velocities generated by the model were compared to empirically based data from a variety of sources, including data generated by Dalla Valle,[1] as a means of testing model validity. Agreement between the theoretical and empirical data varied depending on which data were used but was generally good.

Garrison[8] used a conformal transformation (normally used to obtain the values of the velocity potential for the infinitely long rectangle [slot]) to obtain velocity contours for flanged and unflanged circular openings. His solution included the use of Dalla Valle's centerline velocity[1] to calculate some of the parameters in the equation for the potential. The transformation used is strictly valid for the plain slot (two-dimensional flow) only. Circular openings produce three-dimensional contours. As such, these models would be considered semiempirical.

Flynn and Ellenbecker[9] obtained an analytical solution of Laplace's Equation in cylindrical coordinates for a flanged circular opening. The solution was not adequate in the vicinity of the suction opening. To circumvent this difficulty, Flynn assumed a shape (half-oblate ellipsoids) for the equal velocity surfaces based on Dalla Valle's empirical velocity data. This assumption by Flynn is not necessary because Drkal's work[7] shows that the velocity potential, and hence, the velocity can be calculated at any point.

Esmen et al.[10] more recently applied potential flow theory to derive equations that predict the value of the air velocity at a point in space for single flanged rectangular hoods and for flanged hoods made up of more than one

rectangular opening. The analytical solutions result in very cumbersome equations which become more so as boundary surfaces (or baffles) are added to the space under the influence of the hood(s). Esmen et al.[10] reported very good agreement between theoretical and experimental results.

In summary, past workers have used potential flow theory to derive models for the air velocities induced by infinitely flanged hoods. No purely theoretical models are available for plain hoods (except for the slot) and no general methods are available for complex hoods that are encountered in practice. Past workers also have found that potential flow theory adequately describes the flow into exhaust hoods in general. Good agreement between experimental and theoretical air velocities was observed consistently.

As the geometry of configurations under study becomes more complex, closed-form solutions to Laplace's equation become more difficult to find. In such situations numerical methods of solution are called for. A finite difference method for computing the airflow is presented in this article and was developed using the plain and flanged slot configurations. The method generally is useful for solving problems in which the location and shape of the flow boundary (an equal velocity contour, for example) and the values of the velocity potential or its normal derivative are known there. The method also is useful in solving flow problems in which it is possible to calculate the velocity potential in space from all line or point sinks of which the hood(s) are comprised. The availability of analytical models for the slot facilitates comparison with numerical results.

All computations involving the models presented in this paper were performed on an IBM PC/AT, and the programs were written in Professional Fortran.

A Theoretical Definition of a Slot

Slots are an important class of exhaust openings. They can be thought of as rectangles with a very small AR. In the ACGIH manual,[4] specific applications of the slot configuration have been recommended. These applications include laboratory hoods, welding benches, dip tanks, and degreasers in metal plating operations, *etc.*

The earliest experimental study of a slot was conducted by Silverman.[3] He measured the centerline velocities of flanged slots with AR between 0.017 and 0.2 and plain slots with AR between 0.025 and 0.2. Recent experimental and theoretical work by the authors on centerline models for flanged openings has shown that rectangular hoods behave as slots (centerline velocities equal at a given distance from the face) at AR equal to 0.01 or less.[11] Based on these models, Silverman's models overestimate the velocity at a given distance from the face by as much as 35%. Fletcher's[12] centerline velocity model for the slot is based on data for rectangles with AR of 0.0625 and higher. His model also gives velocities which are higher than those predicted by theory.

Analytical Model for the Plain Slot

The applicability of the potential flow assumption for flow into local exhaust openings implies that the flow is incompressible, inviscid, and irrotational. This also means that Laplace's equation in terms of the velocity potential, ϕ (a complete list of nomenclature and symbols and their definitions is included at the end of this article), applies in the space influenced by the local exhaust opening as follows:

$$\partial^2\phi/\partial x^2 + \partial^2\phi/\partial y^2 = 0 \quad (1)$$

Derivation of a model for the slot starts with finding a conformal transformation which maps the strip ($-\pi <$ Im w $< \pi$) in the w plane into the plain slot of width 2b in the z plane as shown in Figure 1. Im w is the imaginary part of the complex variable w. Such a transformation previously has been derived and involves two successive transformations which are the Shwarz-Christoffel and the exponential transformations.[13,14] The equation relating the variables in the two planes is

$$z = b/\pi(e^w + w + 1) \quad (2)$$

A uniform flow in the strip (w plane) should be equal to the flow in the image plane (z plane). For these flows to be equal, the average velocities in the channel part of the flow must be related as follows:

$$V_{aw} = (b/\pi)\, V_{az} \quad (3)$$

where V_{az} and V_{aw} are the average fluid velocities in the channel part of the flow in the z and w planes, respectively. The complex potential, C_p, in the w plane is given by Equation 4:

$$C_p = V_{aw}\, w \quad (4)$$

It also is given by Equation 5:

$$C_p = \phi + i\psi \quad (5)$$

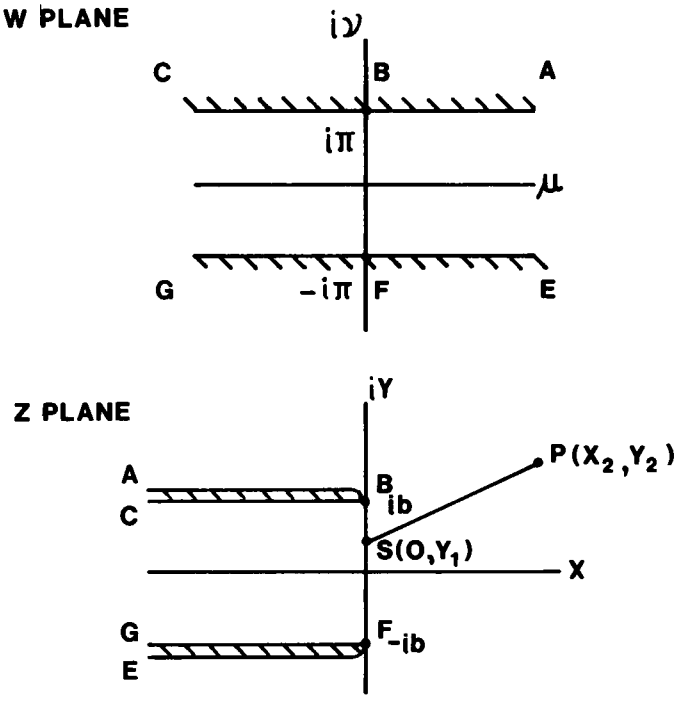

Figure 1—Transformation of a strip into a plain slot

Substituting Equations 3 and 4 into Equation 2 gives

$$z = b/\pi\,[\exp(C_p\pi/V_{az}b) + C_p\pi/V_{az}b + 1] \quad (6)$$

Substituting Equation 5 into Equation 6 and defining the dimensionless variables $\Phi_p = \phi\pi/V_{az}b$; $\Psi_p = \psi\pi/V_{az}b$; $X_p = x\pi/b$; $Y_p = y\pi/b$; $Z_p = z\pi/b$, one obtains a dimensionless form of the transformation.

$$Z_p = \exp(\Phi_p + i\Psi_p) + \Phi_p + i\Psi_p + 1 \quad (7)$$

which, after separation of the real and imaginary components, results in

$$X_p = 1 + \Phi_p + \exp(\Phi_p)\cos\Psi_p \quad (8a)$$

and

$$Y_p = \Psi_p + \exp(\Phi_p)\sin\Psi_p \quad (8b)$$

Equations 8a and b state that for every point (X_p, Y_p) under the influence of the flow into the slot, there is a unique pair of values of Φ_p and Ψ_p. When these are defined for the entire field, the velocity components in the x and y directions at a point are given by

$$u_p = \partial\Phi_p/\partial X_p = 1/V_{az}\,(\partial\phi/\partial x) \quad (9a)$$

and

$$v_p = \partial\Phi_p/\partial Y_p = 1/V_{az}\,(\partial\phi/\partial y) \quad (9b)$$

and the absolute value of the velocity is given by

$$|V| = \sqrt{(u_p^2 + v_p^2)} \quad (10)$$

Velocity contour curves for the plain slot were developed using Equations 8 through 10. A fine grid in the area in front and behind the face was set up. A mesh size of $\pi/20$ gave a density of points that was sufficient to define the individual curves. At each point in the grid, values of Φ_p and Ψ_p were calculated using Equations 8a and 8b by adapting Newton's iterative method.[15]

The equations used in the iteration were as follows:

$$\Phi_p^{i+1} = \Phi_p^i - (fg_s - gf_s)/J \quad (11a)$$

$$\Psi_p^{i+1} = \Psi_p^i - (gf_p - fg_p)/J \quad (11b)$$

where i refers to the iteration number and f and g are obtained by transforming Equation 8 such that

$$f = 1 - X_p + \exp(\Phi_p)\cos\Psi_p + \Phi_p \quad (12a)$$

$$g = \Psi_p - Y_p + \exp(\Phi_p)\sin\Psi_p \quad (12b)$$

f_s and g_s are the partial derivatives of f and g with respect to Ψ_p, while f_p and g_p are the partial derivatives with respect to Φ_p. The Jacobian, J, is given by

$$J = f_p g_s - g_p f_s \quad (13)$$

Implementation of the algorithm involved writing a Fortran program in which approximate values of Φ_p and Ψ_p were calculated at an arbitrary starting point. The approximate values of these were computed by scanning the full range of these two variables (-2.7 to 5.0 and 0 to 3.1416) in the upper half-plane until a combination predicted the starting point within one distance unit. The ranges were determined from plots of constant Ψ_p and Φ_p using Equations 8a and b. Newton's iteration then was applied to the approximate values until convergence was obtained. From then on the values of these variables at one location became the approximate values for the adjacent location on the grid. Point B in Figure 1 is a singular point where the value of the potential is uncertain. Precautions were taken not to use it as a basis for computing points adjacent to it.

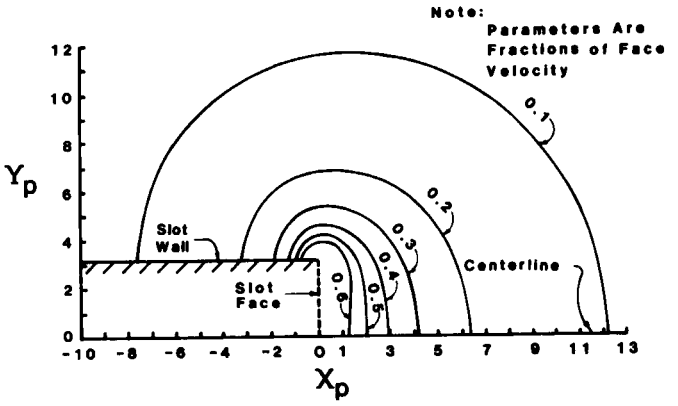

Figure 2—Velocity contours for upper half of plain slot by analytical and numerical solutions

Figure 2 shows the velocity contours that were calculated for the plain slot in the upper half plane. As expected, the curves are perpendicular to both the centerline and the wall, and the airflow across each contour equals the airflow across the face. Therefore, the length of the 10% contour, for example, would be equal to 10 times the length of the face. This is the case for the contours of Figure 2.

Finite Difference Method for Plain Slot

A finite difference approximation of the nondimensionalized form of Equation 1 is the five-point formula which can be used to calculate the potential at a point P in a rectangular grid, shown schematically in Figure 3, in terms of adjacent points as follows[16]:

$$\Phi_P = (\Phi_N + \Phi_E + \Phi_S + \Phi_W)/4 \quad (14)$$

where N, E, S, and W refer to North, South, *etc.*, and the Φ's are dimensionless as before.

Equation 14 holds for interior points in the domain GOABCDE$_2$F shown in Figure 3. For points along DE$_2$, but not including points D and E$_2$, and for points along GOA but not including A or G, the normal derivative $\partial\Phi_P/\partial Y_p$ is zero (no flow across the wall or the centerline) and Equation 14 becomes

$$\Phi_{DE_2} \text{ and } \Phi_{GA} = (2\Phi_N + \Phi_E + \Phi_W)/4 \quad (15)$$

For points along E$_2$F but not including E$_2$ or F

$$\Phi_{E_2F} = (2\Phi_S + \Phi_E + \Phi_W)/4 \quad (16)$$

The equation for point E_2 is given by

$$\Phi_{E_2} = (2\Phi_E + \Phi_{W1} + \Phi_{W2})/4 \quad (17)$$

where Φ_{W1} and Φ_{W2} are the potentials at points west of E_2 along E_2D and E_2F, respectively.

Along FG, but not including the points F and G, the normal derivative $\partial\Phi_P/\partial X_P = 1.0$, which is the mathematical equivalent of saying that along that line the velocity is 100% of the face velocity. This gives

$$\Phi_{FG} = (\Phi_N + 2\Phi_E - 2\Delta X_P + \Phi_S)/4 \quad (18)$$

where ΔX_p is the mesh size in the x direction. It should be mentioned at this point that carrying the solution well into the channel, as opposed to assuming a unit normal derivative at the face, gives a more accurate solution. The normal derivative is unity only in the well developed flow in the channel. A mesh size of $\pi/20$ was found adequate for velocity contour definitions.

At Point G,

$$\Phi_G = (2\Phi_N + 2\Phi_E - 2\Delta X_P)/4 \quad (19)$$

A similar equation may be written for Point F. The potential at points along DC, CB, and BA was calculated using Equations 8a and b.

Equations 14 through 19 may be used to write finite difference equations for each point where the potential is not known. This yields as many simultaneous linear equations as there are unknowns.

Solution of the system of equations was performed using the Gauss-Seidel method which utilizes updated values for adjacent points as soon as these values are available.[15] Successive overrelaxation (SOR) was used to speed up solution of the system of equations. The relaxation factor, ω, was estimated as follows.[17]

$$\omega = 2/(1 + \sqrt{(1 - \rho)}) \quad (20)$$

where ρ is the spectral radius defined as

$$\rho = \lim_{i \to \infty} \Sigma\Delta\Phi^i/\Sigma\Delta\Phi^{i-1} \quad (21)$$

where

$$\Sigma\Delta\Phi^i = |\Phi_1^i - \Phi_1^{i-1}| + |\Phi_2^i - \Phi_2^{i-1}| + \ldots + |\Phi_n^i - \Phi_n^{i-1}| \quad (22)$$

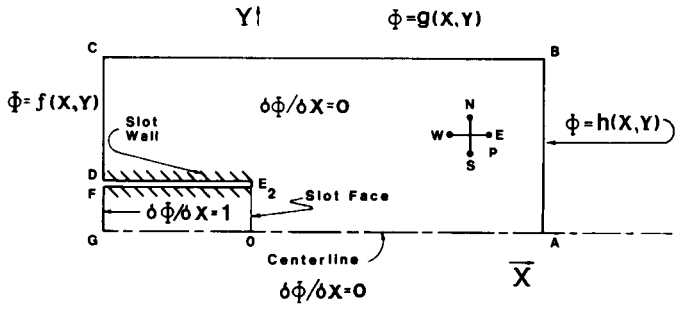

Figure 3—Boundary conditions for numerical solution for upper half of a plain slot

where $\Sigma\Delta\Phi$ is the sum of the absolute value of the differences and the superscript i refers to the iteration number with summation carried out over all points in the domain. An ω value of 1.95 was used in the calculation.

Using SOR, a representative equation for an interior point, P, may be written as follows:

$$\Phi_p^{i+1} = 0.25\omega\,(\Phi_N^{i+1} + \Phi_E^{i+1} + \Phi_S^{i} + \Phi_W^{i}) - (\omega - 1)\,\Phi_p^{i} \quad (23)$$

where i refers to iteration number. Scanning of the grid was from right to left and starting with the mesh point immediately below B in Figure 3. Convergence of the solution was achieved when no significant change in the potential at Point G occurred between iterations.

Velocity contours were developed using Equations 9 and 10. The components of velocity were calculated using central differences such that $u_P = \partial\Phi_p/\partial X_p = (\Phi_E - \Phi_W)/2\,\Delta X_p$. The contours obtained in this manner were identical to those obtained using the analytical model described earlier and shown in Figure 2.

Comparison of Experimental and Theoretical Data for Plain Slot

Following Tyaglo and Shepelev,[6] who used centerline velocity measurements as a check on their model for the rectangle, measurements of centerline velocities (as fraction of face velocity), V_{CLP}, were made. Data also were taken to compare theoretical and experimental values of the velocity contour which corresponds to 10% of the average velocity in the channel (face velocity). This corresponds to the curve with parameter of 0.1 in Figure 2.

Experimental centerline velocity data (V_{CLP}) were obtained for a rectangular opening of AR = 0.01 with dimensions of 1.22 cm by 121.92 cm (0.48 in. by 48 in.). A hot wire anemometer (TSI Model 1051-2, TSI, Inc., St. Paul, Minn.), interfaced to an Apple IIe microcomputer through an AI13 analog-to-digital converter, was used. The anemometer was calibrated in a wind tunnel (Series 400 air velocity calibration system, Kurz Instruments, Inc., Carmel Valley, Calif.). A laser beam was used to align the anemometer probe with the centerline of the opening. The average face velocity was determined by pitot-tube traverses of the 8 in. circular duct through which air exhausted from the slot passed. Velocity data were taken at distances between 0.5 in. and 7 in. from the hood face. The theoretical and experimental values are compared in Table I. The data are reported as a fraction of the average velocity in the channel. A plot of the data appears in Figure 4. A statistical t-test was applied to each pair of theoretical and experimental values to determine whether the differences between them were significantly different from zero.[18] The test showed no significant difference at the 5% level of significance. This indicates good agreement between the theoretical model and experimental centerline data.

Comparison of experimental and theoretical values for the 10% contour was performed by taking four values of velocity at four different x locations which bracket the 10% value, for each y level studied. The data are presented in Table II. The x coordinate for each y value where the veloc-

TABLE I
Theoretical and Experimental Centerline Velocities for the Plain Slot

Distance		Centerline Velocity, V_{CLP}[A]		
x (in.)	X_p	Theoretical	Experimental[B]	% Difference
0.50	6.54	0.1948	0.2065	- 5.7
0.75	9.82	0.1267	0.1348	- 6.0
1.00	13.09	0.0925	0.0970	- 4.6
1.50	19.63	0.0593	0.0659	-10.0
2.00	26.18	0.0433	0.0438	- 1.1
3.00	39.27	0.0280	0.0248	12.9

[A]Velocity as fraction of face velocity in the channel
[B]Face velocity was 3212 fpm.

ity was exactly 10% of the face velocity then was computed by inverse interpolation from the four values of velocity.[15] The experimental and theoretical values of the coordinates for the 10% contour are plotted in Figure 5. The agreement generally was good. Some points departed slightly from the theoretical line, however, because the velocity measuring probe used was highly directional and because the range of distances was small.

Analytical Model for Flanged Slot

An analytical model for the flow into a flanged slot may be derived using the same method presented earlier for the plain slot (Equations 8a and b). Such a model has been in existence for some time, and Heinsohn[5] used it when he studied the capture characteristics of this configuration. In what follows, however, an analytical model will be developed which utilizes the principle that for infinitely flanged openings, in general, it is possible to compute the velocity potential at a point in space. This implies that the normal derivative at the face of the hood is one. While this is strictly not true, the assumption causes no problems in computing the air velocity at locations of practical significance, *i.e.*, those away from the face. The derivation to follow is a general extension of a method used by the authors to derive expressions for centerline velocities.[11]

A flanged slot would be obtained by erecting a boundary surface along the y axis of the plain slot in Figure 1. The face of the slot may be thought of as consisting of many line sinks, such as the one passing through Point S. Assuming an even distribution of line sinks across the face an expression for the velocity potential at the field Point P may be derived as follows.

A line sink at S for the flanged slot generates a semicylindrical equipotential surface. The velocity V_F at Point P, therefore, is

$$V_F = q/\pi Lr \qquad (24)$$

where q is the suction flow through the line sink, r is the distance between P and S, and L is the length of the sink (in a direction perpendicular to the x-y plane). The velocity V_F is the derivative of the velocity potential with respect to r ($d\phi_{FP}/dr$) and $q = Qdy_1/2b$ where Q is the total suction flow through the slot and dy_1 is the width of the line sink.

Before proceeding any further, it would be useful to introduce the dimensionless variables $R = r/b$; $Y_1 = y_1/b$; $X_2 = x_2/b$; $Y_2 = y_2/b$; and $\Phi_{FP} = \phi_{FP}A/bQ$. A is the area of the slot and Φ_{FP} is the velocity potential at Point P for the flanged slot. Equation 24 then becomes

$$d\Phi_{FP}/dR = 1/(Q/A)\, d\phi_{FP}/dr = dY_1/\pi R \qquad (25)$$

Therefore the velocity potential at Point P, because of all line sinks forming the slot, becomes

$$\Phi_{FP} = 1/\pi \int_{-1}^{1} \ln R \, dY_1 \qquad (26)$$

Since $R = \sqrt{[(Y_2 - Y_1)^2 + X_2^2]}$ and the components of velocity, as fractions of face velocity, in the X and Y directions are given by $u_{FP} = \partial\Phi_{FP}/\partial X_2$ and $v_{FP} = \partial\Phi_{FP}/\partial Y_2$, the

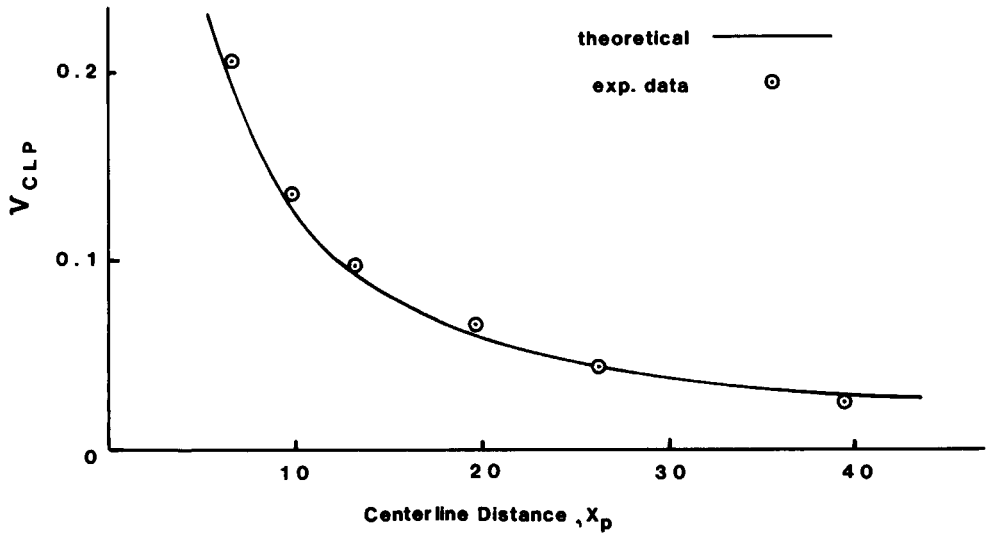

Figure 4—Centerline velocity versus distance for the plain slot

TABLE II
Air Velocity, as Fraction of Face Velocity, at Various Locations for Plain Slot

y (in.)	x (in.) (underlined)			
0.000	x_1 = 0.750	x_2 = 1.000	x_3 = 1.250	x_4 = 1.500
	0.1315	0.0967	0.0759	0.0636
0.250	x_1 = 0.750	x_2 = 1.000	x_3 = 1.250	x_4 = 1.500
	0.1140	0.0878	0.0710	0.0594
0.500	x_1 = 0.750	x_2 = 1.000	x_3 = 1.250	x_4 = 1.500
	0.1092	0.0856	0.0702	0.0584
0.750	x_1 = 0.500	x_2 = 0.750	x_3 = 1.000	x_4 = 1.250
	0.1062	0.0874	0.0738	0.0691
0.750	x_1 = -0.125	x_2 = -0.250	x_3 = -0.375	x_4 = -0.500
	0.1413	0.1257	0.1068	0.0918

following expression for the components may be obtained after partial differentiation of lnR with respect to X_2 and Y_2, respectively, and completing the integration with respect to Y_1.

$$u_{FP} = 1/\pi\,[\tan^{-1}(1 - Y_2)/X_2 + \tan^{-1}(1 + Y_2)/X_2] \quad (27a)$$

$$v_{FP} = 1/2\pi \ln[(Y_2 + 1)^2 + X_2^2]/[(Y_2 - 1)^2 + X_2^2] \quad (27b)$$

Finite Difference Method for Flanged Slot

The numerical solution for this configuration parallels that of the plain slot. Equation 14 applies to interior Points P as shown in Figure 6.

For points along CD, but not including Points C and D, the normal derivative $\partial\Phi_{FP}/\partial X_2$ is zero (no flow across the flange), and Equation 14 becomes

$$\Phi_{CD} = (\Phi_N + 2\Phi_E + \Phi_S)/4 \quad (28)$$

Along DO, but not including the D and O, the normal derivative $\partial\Phi_{FP}/\partial X_2$ may be assumed to be unity without too much loss of accuracy at points away from the face. This gives

$$\Phi_{DO} = (\Phi_N + 2\Phi_E - 2\Delta X_2 + \Phi_S)/4 \quad (29)$$

where ΔX_2 is the mesh size in the x direction. A mesh size of 0.1 was found adequate for velocity contour definitions. At Point D the normal derivative changes abruptly from 0 to 1, resulting in a singularity. Accuracy of the entire solution will depend upon how the singularity is handled. The best solution was obtained when the normal derivative at Point D was assumed to be 0.5—the average of the value at points below and above. The coefficient of ΔX_2 in Equation 29, therefore, will be 1 instead of 2.

At point O, the intersection between the slot face and the centerline,

$$\Phi_0 = (2\Phi_N + 2\Phi_E - 2\Delta X_2)/4 \quad (30)$$

Along the centerline OA, but not including A, the normal derivative $\partial\Phi_{FP}/\partial Y_2$ is zero (because of no flow across the centerline), yielding

$$\Phi_{OA} = (2\Phi_N + \Phi_E + \Phi_W)/4 \quad (31)$$

Along the free boundary of the rectangular grid (ABC), the potential is calculated using Equation 25 which, when the integrals are set up, may be written as

$$\Phi_{ABC} = 1/\pi \int_a^{R_{max}} \int_{-1}^{1} dR\, dY_1/R \quad (32)$$

where R_{max} represents the distance from the line sink to the point at which the potential is calculated and a is an arbitrary constant with R and Y_1, as before. In the actual calculations, the value of a used was 0.5; however, because only a relative value of the potential is of interest, a could be any number greater or smaller than 0.5.

Solution of the system of equations was performed as before for the plain slot. SOR was implemented as given in Equations 20 and 23.

Scanning of the grid was from right to left and started with the mesh point immediately below B in Figure 6. Covergence of the solution was achieved when no significant change in the potential at Point O occurred between iterations.

The velocity at each point was calculated as was done for the plain slot. Contour plots generated using the analytical solution (Equation 27) and the numerical solution are shown in Figure 7. It may be seen that contours from both methods diverge slightly, but in all cases the same shapes are generated.

Comparison of Experimental and Theoretical Velocity Data for Flanged Slot

The applicability of the assumption of potential flow into infinitely flanged rectangular hoods was tested experimen-

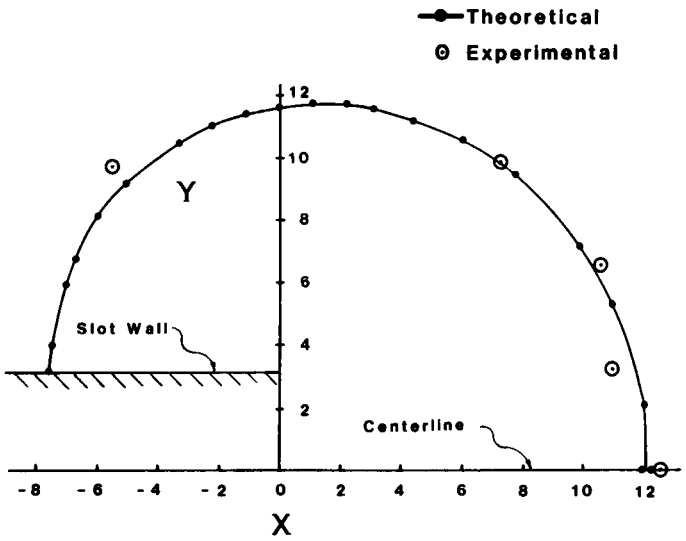

Figure 5—Plot of theoretical and experimental data for 10% velocity contour for plain slot

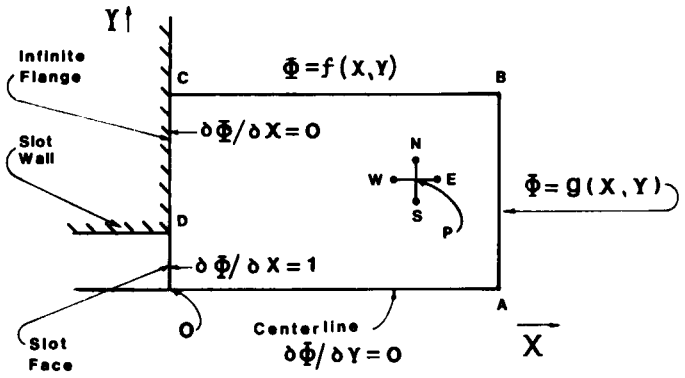

Figure 6—Boundary conditions for numerical solution for upper half of a flanged slot

tally by other workers.[6-11] Esmen et al.[10] presented a plot in which the theoretical and experimental values of air velocity were correlated for flanged rectangles. Agreement between these values was within 15%. The location of the points, however, was not reported. It should be stated here that experimental validation of the flow into one configuration implies applicability of the assumption of potential flow for other configurations since the same principles are used in model derivation. In what follows, a comparison between theoretical and experimental centerline velocities will be provided for the flanged slot.

An analytical model for the centerline velocities (as fraction of face velocity), V_{CLF}, was derived from Equation 27a by setting $Y_2 = 0$. Then

$$V_{CLF} = (2/\pi) \tan^{-1} (1/X_2) \quad (33)$$

Experimental data on centerline velocities were obtained in a similar manner as for the plain slot. A Kurz model 1440 anemometer was used to obtain the data, however. The experimental centerline data and the corresponding theoretical values calculated using Equation 33 are given in Table III and plotted in Figure 8. A statistical t-test showed no significant difference between the paired data (theoretical and experimental values at each point) at the 1% level of significance.[18] This indicates good agreement between analytical and experimental centerline data. A few centerline values, predicted by the numerical method, also are plotted in Figure 8. Good agreement with previously discussed data was observed.

Conclusions

Experimental work by the authors and by others has shown that the assumption of potential flow closely approximates actual conditions of airflow into local exhaust hoods. This implies the applicability of Laplace's equation in terms of the velocity potential. Closed-form solutions to Laplace's equation exist for plain slots and for infinitely flanged slots, rectangles, and circles. These are some of the situations in which it is possible to calculate the velocity potential at a point in space.

Closed-form analytical solutions are available for relatively few exhaust hood configurations. Numerical methods of solving for the flow are indicated for the general case in which the location and shape of the flow boundary and the boundary conditions are known. A finite difference method is presented in this article and was applied successfully to computing the flow into plain and flanged slots. The availability of analytical solutions for these configurations permitted comparison with the numerical solutions.

The numerical solution for the plain slot was found to be identical to the analytical one. For the flanged slot, the numerical solution slightly overestimated the analytical, but agreement generally was good.

Acknowledgment

Excellent help with experimental measurements was provided by Ova Johnston. Daniel Watkins ably built the configurations studied.

Nomenclature

A	Area of slot (2bL)
AR	Aspect ratio—ratio of width to length of a rectangle
b	Half of slot width
C_p	The complex potential in z plane for the plain slot
f, f_p, f_s	Function of Φ and Ψ and its derivatives with respect to Φ (f_p) and Ψ (f_s) used in Newton's method for plain slot
g, g_p, g_s	Function of Φ and Ψ and its derivatives with respect to Φ (g_p) and Ψ (g_s) used in Newton's method for plain slot
J	Jacobian
L	Length of slot
q	Flow through a line sink at the face of a flanged slot
Q	Flow into slot
r	Distance from origin to point x, y in space for flanged slot
R	Dimensionless r (r/b)
R_{max}	Distance from the line sink to the point (x, y) at which the potential is calculated for flanged slot

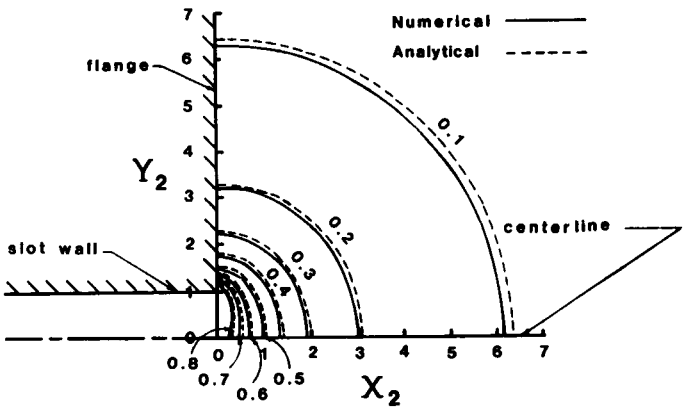

Figure 7—Upper half of contours for flanged slot by numerical and analytical methods

TABLE III
Comparison of Experimental and Theoretical Centerline Velocities for Flanged Slot

Distance		Centerline Velocities, V_{CLF}[A]		
x (in.)	X_2	Analytical[B]	Experimental[C]	% Difference
0.5	2.08	0.285	0.264	- 8.0
1.0	4.17	0.153	0.148	- 3.4
1.5	6.25	0.101	0.097	- 4.1
2.0	8.33	0.076	0.071	- 7.0
2.5	10.42	0.061	0.055	-10.9
3.0	12.50	0.051	0.049	- 4.1
4.0	16.67	0.038	0.035	- 8.6
5.0	20.83	0.030	0.028	- 5.7
6.0	25.00	0.025	0.025	0.0

[A]As fraction of face velocity
[B]Equation 27
[C]Face velocity 3212 fpm

u_p, u_{fp} Velocity component in x direction as fraction of average velocity in the channel for plain and flanged slots, respectively

V_{aw}, V_{az} Average fluid velocity in the channel in the w and z planes, respectively

v_p, v_{fp} Velocity component in y direction as fraction of average velocity in the channel for plain and flanged slots, respectively

V_{CLF}, V_{CLP} Centerline velocities as fraction of average velocity in the channel for flanged and plain slots, respectively

V_F Velocity at a point in space for flanged slot

$|V|$ Magnitude of velocity at a point

w Complex number in the w plane with coordinates ν and μ

x_2 Distance in the x direction from hood face to a point in space for flanged slot

X_p, X_2 Dimensionless distances in the x direction for plain slot ($x\pi/b$) and for flanged slot (x_2/b), respectively

y_1 Distance from origin to some point y on face of flanged slot

Y_1 Dimensionless distance (y_1/b)

Y_p, Y_2 Dimensionless distance in y direction for plain slot ($y\pi/b$) and for flanged slot (y_2/b), respectively

z Complex number in the z plane with coordinates x, y

Z_p Dimensionless complex number in the z plane ($z\pi/b$)

Greek Symbols

ψ Stream function at a point in space for plain slot

Ψ Dimensionless stream function for plain slot ($\psi\pi/V_{az}b$)

ϕ Velocity potential at a point in space

Φ_p, Φ_{FP} Dimensionless velocity potential for plain slot ($\phi\pi/V_{az}b$) and flanged slot ($\phi_{FP}A/bQ$) respectively

Φ_N, Φ_E, Φ_S, Φ_W Dimensionless velocity potentials used in finite difference solution of Laplace's equation (subscripts refer to points north, east, south, and west of point on the computational grid)

ω Overrelaxation factor

ρ Spectral radius of the numerical solution by successive overrelaxation

ΔX_p Differential x distance for numerical solution of plain slot

ΔX_2 Differential x distance for numerical solution of flanged slot

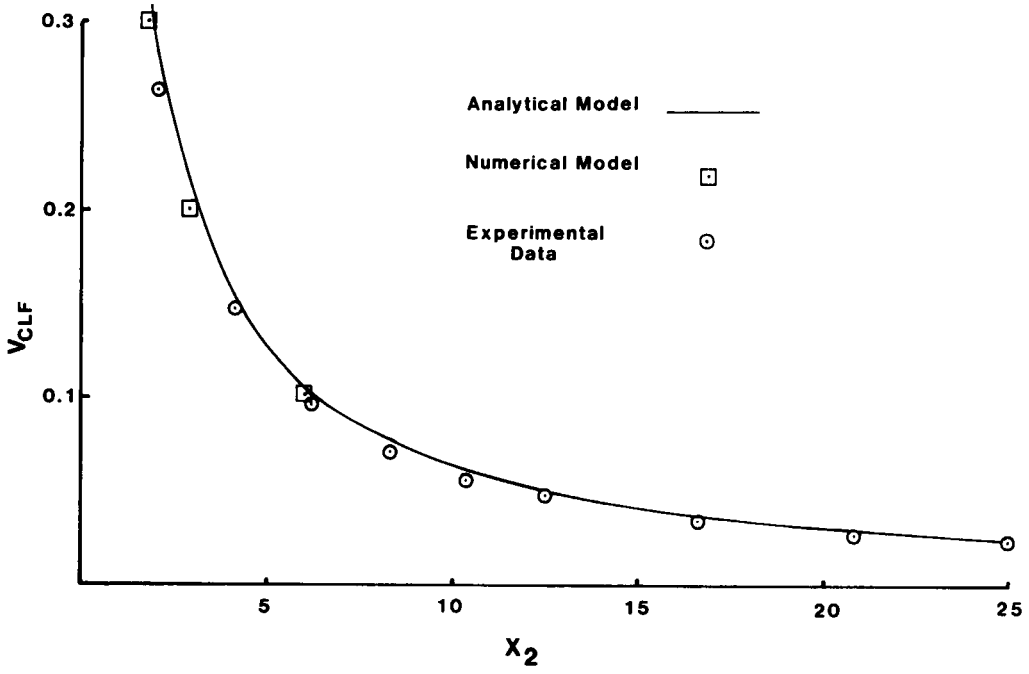

Figure 8—Plot of experimental and theoretical centerline velocities for flanged slot

References

1. **Dalla Valle, J.M.:** *Exhaust Hoods.* 2d ed. New York: The Industrial Press, 1952.
2. **Silverman, L.:** Centerline Velocity Characteristics of Round Hoods under Suction. *J. Ind. Hyg. Toxicol. 24*:259-266 (1942).
3. **Silverman, L.:** Centerline Velocity Characteristics of Narrow Exhaust Slots. *J. Ind. Hyg. Toxicol. 24*:267-276 (1942).
4. **American Conference of Governmental Industrial Hygienists:** *Industrial Ventilation—A Manual of Recommended Practice.* 19th ed. Lansing, Mich.: American Conference of Governmental Industrial Hygienists, 1986. pp. 4-1-4-7.
5. **Heinsohn, R.J.:** Advanced Design Methods in Industrial Ventilation. In *Ventilation '85,* edited by H.D. Goodfellow. Amsterdam, Holland: Elsevier Science Publishers, 1986. pp. 81-109.
6. **Tyaglo, I.G. and I.A. Shepelev:** Dvizhenie vozdushnogo potoha k vytyazhnomu otverstiyu [Movement of Airflow to a Suction Opening]. *Vodosnabzh. Sanit. Tekh. 5*:24-25 (1970). [In Russian].
7. **Drkal, F.:** Stromungsverhaltnisse bei runden Saugoffnungen mit Flansch [Theoretical Solution—Flow Conditions for Round Suction Openings with a Flange]. *HLH, Z. Heiz. Luft., Klimatech., Haustech. 21(8)*:271-273 (1970).
8. **Garrison, R.P.:** Velocity Calculation for Local Exhaust Inlet—Graphical Design Concepts. *Am. Ind. Hyg. Assoc. J. 44*:941-947 (1983).
9. **Flynn, M.R. and M.J. Ellenbecker:** The Potential Flow Solution for Air Flow into a Flanged Circular Hood. *Am. Ind. Hyg. Assoc. J. 46*:381-322 (1985).
10. **Esmen, N.A., D.A. Weyel, and F.P. McGuigan:** Aerodynamic Properties of Exhaust Hoods. *Am. Ind. Hyg. Assoc. J. 47*:448-454 (1986).
11. **Anastas, M.Y. and R.T. Hughes:** Centerline Velocity Models for Flanged Local Exhaust Openings. *Appl. Ind. Hyg. 3*:342-347 (1988).
12. **Fletcher, B.:** Centerline Velocity Characteristics of Rectangular Unflanged Hoods and Slots Under Suction. *Ann. Occup. Hyg. 20*:141-146 (1977).
13. **Hayashi, T., R.H. Howell, M. Shibata, and K. Tsuji:** *Industrial Ventilation and Air Conditioning.* Boca Raton, Fla.: CRC Press, Inc., 1985. pp. 5-7.
14. **Silverman, R.A.:** *Complex Analysis with Applications.* Englewood Cliffs, N.J.: Prentice-Hall, Inc., 1974. pp. 223-224.
15. **Conte, S.D.:** *Elementary Numerical Analysis.* New York: McGraw-Hill Book Co., 1965. pp. 45-46.
16. **Ames, W.F.:** *Numerical Methods for Partial Differential Equations.* 2d ed. Orlando, Fla.: Academic Press, Inc., 1977. pp. 15-19.
17. **Smith, G.D.:** *Numerical Solution of Partial Differential Equations.* New York: Oxford University Press, 1965. pp. 150-151.
18. **Kennedy, J.B. and A.M. Neville:** *Basic Statistical Methods for Engineers and Scientists.* New York: IEP (A Dun-Donnelley Publisher), 1976. pp. 210-213.

8 February 1988; Revised 3 April 1989